JOURNAL OF GUIDANCE, CONTROL, AND DYNAMICS
Vol. 29, No. 1, January–February 2006

Closed-Loop Aeromechanical Stability of Hingeless Rotor Helicopters with Higher Harmonic Control

Marco Lovera* and Patrizio Colaneri†
Politecnico di Milano, 20133 Milan, Italy
and
Carlos Malpica‡ and Roberto Celi§
University of Maryland, College Park, Maryland 20742

The development of a state-space formulation for a multi-input/multi-output (MIMO) higher-harmonic-control (HHC) system is described. Results are also presented of a numerical investigation into closed-loop performance and stability of an HHC system, implemented in the rotating system, based on the simulation of a hingeless rotor helicopter. The results show that the HHC controller reduces the 4/rev accelerations at the center of gravity. The percentage reductions obtained in the simulations are in excess of 80–90%. The vibration attenuation occurs within 5–7 s after the HHC system is turned on. This is equivalent to a frequency of around 1 rad/s, where flight control systems and human pilots tend to operate. Therefore, interactions and potential adverse effects on the stability and control characteristics of the helicopter should be explored. The HHC problem is intrinsically time periodic if the HHC inputs include frequencies other than the frequency one wishes to attenuate. This is true even if the rest of the model is assumed to be time invariant. In these cases, the closed-loop stability results obtained using constant coefficient approximations can be incorrect even at lower values of the advance ratio μ, where constant coefficient approximations of the open-loop dynamics are accurate.

Nomenclature

$A(t)$	=	open-loop stability matrix
A_0	=	stability matrix (constant approximation)
B	=	number of blocks in the harmonic transfer function
$B(t)$	=	input (control) matrix
$C(t)$	=	output (measurement) matrix
C_T	=	rotor thrust coefficient
$D(t)$	=	direct input/output matrix
J	=	performance index for the higher-harmonic-control (HHC) control law
K	=	Gain of HHC controller
m	=	number of control inputs
N	=	number of rotor blades
n	=	number of measured outputs
n_s	=	system order
p	=	number of measured outputs
Q	=	output weighting matrix in performance index J
R	=	control effort weighting matrix in performance index J
r	=	tuning parameter in HHC performance index
T	=	rotor revolution period
t	=	time
$\boldsymbol{u}$	=	input vector
$\boldsymbol{y}$	=	output vector
ψ	=	azimuth angle of reference blade, $=\Omega t$
Ω	=	rotor angular velocity

Received 29 January 2004; revision received 7 October 2004; accepted for publication 12 October 2004.

*Associate Professor, Dipartimento di Elettronica e Informazione; lovera@elet.polimi.it.

†Professor, Dipartimento di Elettronica e Informazione; colaneri@elet.polimi.it.

‡Graduate Research Assistant, Department of Aerospace Engineering; cmalpica@eng.umd.edu.

§Professor, Department of Aerospace Engineering; celi@eng.umd.edu. Senior Member AIAA.

Introduction

HIGHER harmonic control (HHC) and individual blade control (IBC) have been considered for many years as a viable approach for the design and the implementation of active rotor control laws aiming at the attenuation of helicopter vibrations (e.g., see the survey papers.[1,2] The main idea of HHC and IBC is to try to attenuate N/rev vibratory components in the fuselage accelerations (N being the number of rotor blades) or in the rotor hub loads by adding suitably phased N/rev and other components to the rotor controls, either in the fixed (HHC) or rotating (IBC) frame. A number of studies have been carried out to determine the feasibility of active vibration control both from the theoretical and the experimental point of view; in particular, as far as the analysis of the dynamic behavior of the single-input/single-output (SISO) HHC is concerned, a fundamental result was given in Ref. 3, where a continuous time analysis of HHC was carried out for the first time, and it was shown that, to first approximation, the classical T-matrix HHC algorithm (Ref. 4) can be written as a linear time-invariant dynamic compensator. More recently, however, it has been proposed to achieve the attenuation of N/rev vibrations by means of lower frequency inputs, such as, for example, 2/rev or 3/rev for a four-bladed rotor. To this purpose, a generalization of the T-matrix algorithm has been proposed in the literature (Ref. 5), but no detailed theoretical analysis of that approach has been carried out so far. As the just-mentioned generalization of the T-matrix algorithm turns out to be a linear time-periodic compensator, we will refer to it as the periodic HHC (PHHC) algorithm. Therefore, both the HHC and the PHHC algorithms call for the use of periodic systems theory[6] for closed-loop stability and performance analysis.

Although the literature on helicopter vibration control using HHC and IBC is very extensive, there are relatively few studies that address the issue of the stability of an HHC/IBC system. In an early, comprehensive study, Johnson[7] studied the open- and closed-loop stability of several types of deterministic and adaptive controllers, including online estimation of the T matrix. Gupta and Du Val[8] and Du Val et al.[9] studied the coupled rotor-fuselage stability of a helicopter with HHC. The closed-loop stability analysis, which was limited to a constant-coefficient helicopter model and to a hover flight condition, indicated that HHC had beneficial effects on rigid-body stability, but only if rotor state feedback were included. McKillip's study of IBC using periodic control techniques[10]

included the calculation of Floquet characteristic exponents for the closed-loop stability evaluation of a flapping blade model. The controller operated in the time domain, that is, its output was not limited to harmonics of the rotor frequency. The closed-loop poles were always stable. The stability of a fixed T-matrix HHC algorithm was studied by Hall and Wereley,[3,11] who concluded that both the continuous- and the discrete-time HHC algorithms are quite robust with respect to modeling errors. More recently, Cheng et al.[12] have presented a methodology for the derivation of approximate linearized, time-invariant, state-space models of helicopters and have examined the interaction between HHC and FCS. A Sikorsky UH-60 configuration was used in the study. Although the closed-loop stability not explicitly studied, for example, in the form of stability eigenvalues, Bode plots of response to harmonic inputs provided information on gain and phase margins and disturbance rejection characteristics. Finally, Patt et al.[13] have recently presented a detailed convergence and robustness theoretical analysis of two HHC schemes and have provided stability bounds essentially related to the accuracy of the T matrix.

This brief literature survey shows that very limited attention has been devoted to one key aspect of the problem, namely, the closed-loop stability of a helicopter with HHC/IBC, as opposed to just the stability of the HHC algorithm itself. With the partial exception of Refs. 8 and 9, rotor and fuselage dynamics have always been taken into account only approximately, through the T matrix, and therefore through a quasi-static representation of the relationship between the harmonics of the input and those of the output. As a consequence, some important practical questions on closed-loop aeroelastic stability are currently unanswered. For example, there is no published information on whether an HHC/IBC system can destabilize the regressive lag mode of a hingeless or bearingless rotor helicopter. Furthermore, the role of periodicity in determining the actual closed-loop dynamics still has to be fully assessed.

In the light of the preceding remarks, the objectives of this paper are the following: 1) to provide a simple state-space derivation for the continuous time form of the SISO HHC compensator (input and output at the same rotor harmonic), first introduced in Ref. 3; 2) to demonstrate how the same approach can be used to work out a state-space representation for the SISO PHHC compensator (input and output at different rotor harmonics), which is suitable for closed-loop stability and robustness analysis; 3) to generalize the preceding results to get to a general approach for the derivation of the state-space form for a multi-input/multi-output (MIMO) HHC controller (any combinations of harmonics for inputs and outputs); and 4) to present the results of a numerical investigation into the closed-loop stability properties of higher harmonic control, based on a simulation study of the coupled rotor-fuselage dynamics of a four-bladed hingeless rotor helicopter. (Note that some preliminary results have been presented in Ref. 14).

The main significance of the present work is that it addresses the question of whether the presence of a closed-loop HHC will affect the aeroelastic stability of a coupled rotor-fuselage system. Although some partial answers could obviously be extracted from the analysis of transient time histories, no suitable methodology to answer this question directly is available in the published literature.

Helicopter Simulation Model

The baseline simulation model used in this study is a non-real-time, blade-element type, coupled rotor-fuselage simulation model (see Ref. 15 for details). The fuselage is assumed to be rigid and dynamically coupled with the rotor. A total of nine states describe fuselage motion through the nonlinear Euler equations. Fuselage and blade aerodynamics are described through tables of aerodynamic coefficients, and no small angle assumption is required. A coupled flap-lag-torsion elastic rotor model is used. Blades are modeled as Bernoulli–Euler beams. The rotor is discretized using finite elements, with a modal coordinate transformation to reduce the number of degrees of freedom. The elastic deflections are not required to be small. Blade-element theory is used to obtain the aerodynamic characteristics on each blade section. Quasi-steady aerodynamics is used, with a three-state dynamic inflow model. Linearized models are extracted numerically, by perturbing rotor, fuselage, and inflow states about a trimmed equilibrium position. Because the equations of the coupled rotor/fuselage dynamics are written in the fixed frame of reference, the linearized models turn out to be time-periodic with period T/N, where N is the number of blades and T is the period of one rotor revolution. Note that in the following the azimuth angle $\psi = \Omega t$ will be used as an independent variable.

The matrices of the linearized model are generated as Fourier series. For example, the state matrix $A(\psi)$ is given as

$$A(\psi) = A_0 + \sum_{k=1}^{K} [A_{\mathrm{kc}} \cos(kN\psi) + A_{\mathrm{ks}} \sin(kN\psi)] \qquad (1)$$

where the matrices A_0, A_{kc}, and A_{ks} are constant, and only A_0 is retained for constant coefficient approximations.

Similarly, the control matrix $B(\psi)$ is obtained assuming for the pitch control of each blade the form

$$\theta_i(\psi) = \theta_0 + \sum_{k=1}^{K} \left[\theta_{\mathrm{kc}} \cos\left(\psi + \frac{2\pi}{N} i\right) + \theta_{\mathrm{ks}} \sin\left(\psi + \frac{2\pi}{N} i\right) \right] \qquad i = 0, \ldots, N-1 \quad (2)$$

where i is the blade number and K is the total number of input harmonics. The rotor input vector $\boldsymbol{u}$ used in the present study is

$$\boldsymbol{u} = [\theta_0 \quad \theta_{1c} \quad \theta_{1s} \quad \theta_{3c} \quad \theta_{3s} \quad \theta_{4c} \quad \theta_{4s} \quad \theta_{5c} \quad \theta_{5s}]^T \qquad (3)$$

therefore, for the four-bladed rotor considered in this study, the higher harmonic input is composed of the $N-1$/rev, N/rev, and $N+1$/rev harmonics. For simplicity, the tail rotor collective input θ_{0t} is omitted from all of the equations of this paper, but it is obviously included in the actual mathematical model.

As Eq. (2) shows, the higher harmonic control is applied in the rotating system. Therefore, although the control is identical for all blades at the same azimuth angle, this arrangement is what is often defined as IBC. However, it should be pointed out that although HHC and IBC represent significantly different technologies from the implementation point of view (e.g., choice of actuators and sensors), they are completely equivalent from the control theoretic point of view.

Finally, the trim procedure is the same as in Ref. 16. The rotor equations of motion are transformed into a system of nonlinear algebraic equations using a Galerkin method. The algebraic equations enforcing force and moment equilibrium, the Euler kinematic equations, the inflow equations, and the rotor equations are combined in a single coupled system. The solution yields the harmonics of a Fourier expansion of the rotor degrees of freedom, the pitch control settings, trim attitudes and rates of the entire helicopter, and main and tail rotor inflow. During the trim calculations the HHC system is turned off.

State-Space Formulation of Higher Harmonic Controllers

This section presents the derivation of the state-space formulation of a MIMO HHC controller in which inputs and outputs can be at arbitrary multiples of the fundamental rotor frequency. This is done by building state-space formulations of HHC controllers of increasing complexity. After some background on the T-matrix algorithm, a continuous-time, state-space analysis is presented for the case of a SISO HHC system in which input and output are at the same harmonic (in this case, N/rev). Next, the analysis is extended to the case in which input and output are at different harmonics. Finally, the case of the MIMO HHC system with inputs and outputs at arbitrary harmonics is considered, by combining the results of the two previous cases. More precisely, the following three cases, corresponding to three different selections for the control input vector $\boldsymbol{u}$, will be considered: 1) control input given by a single harmonic at the blade passing frequency N/rev:

$$\boldsymbol{u} = \boldsymbol{u}_N = [\theta_{\mathrm{Nc}} \quad \theta_{\mathrm{Ns}}]^T$$

2) control input given by a single harmonic at a frequency M/rev different from N/rev:

$$\boldsymbol{u} = \boldsymbol{u}_M = [\theta_{\mathrm{Mc}} \quad \theta_{\mathrm{Ms}}]^T$$

3) control input given by the superposition of a number of different harmonics, such as, for example,

$$u = [\theta_{(N-1)c}\theta_{(N-1)s} \quad \theta_{\mathrm{Nc}}\theta_{\mathrm{Ns}} \quad \theta_{(N+1)c}\theta_{(N+1)s}]^T \tag{4}$$

For the purpose of the present study, only fixed parameters HHC will be considered, that is, the T matrix will be fixed and not adaptive. Also, the stability analysis will be carried out in continuous time: the role of digital implementation on the stability and performance of the HHC loops will be investigated in future work.[17]

Basic T-Matrix Algorithm

A typical nonadaptive HHC system is based on a discrete-time mathematical model describing the response of the helicopter to higher harmonic inputs, of the general form

$$\boldsymbol{y}_N(k) = T_{N,N}\boldsymbol{u}_N(k) + \boldsymbol{y}_{0N}(k) \tag{5}$$

where k is the rotor revolution index, $\boldsymbol{y}_N$ is a vector of N/rev harmonics of measured outputs (e.g., hub loads or accelerations at some point of the fuselage), $\boldsymbol{u}_N$ is a vector of control inputs, and $T_{N,N}$ is a 2×2 constant matrix. The vector $\boldsymbol{y}_N(k)$ is defined as

$$\boldsymbol{y}_N(k) = \begin{bmatrix} \boldsymbol{y}_{\mathrm{Nc}}(k) \\ \boldsymbol{y}_{\mathrm{Ns}}(k) \end{bmatrix} = \begin{bmatrix} \dfrac{1}{\pi}\displaystyle\int_{k\pi}^{(k+1)\pi} \boldsymbol{y}(\psi)\cos(N\psi)\,\mathrm{d}\psi \\ \dfrac{1}{\pi}\displaystyle\int_{k\pi}^{(k+1)\pi} \boldsymbol{y}(\psi)\sin(N\psi)\,\mathrm{d}\psi \end{bmatrix} \tag{6}$$

The vector $\boldsymbol{y}_{0N}$ contains the N/rev harmonics of the baseline vibrations, that is, the vibrations in the absence of HHC. In practical applications, $\boldsymbol{y}_N$ is typically the output of a digital or analog harmonic analyzer. The control input vector is similarly defined as

$$\boldsymbol{u}_N = \begin{bmatrix} \theta_{\mathrm{Nc}} \\ \theta_{\mathrm{Ns}} \end{bmatrix} \tag{7}$$

where θ_{Nc} and θ_{Ns} are, respectively, the cosine and sine components of the N/rev pitch control input, applied in the rotating system.

The HHC inputs are generally updated at discrete-time intervals, for example, once per rotor revolution. The conventional HHC control law is derived by minimizing at each discrete time step k the cost function

$$J(k) = \boldsymbol{y}_N(k)^T Q \boldsymbol{y}_N(k) + \Delta\boldsymbol{u}_N(k)^T R \Delta\boldsymbol{u}_N(k) \tag{8}$$

where $Q = Q^T \geq 0$, $R > 0$, and $\Delta\boldsymbol{u}_N(k)$ is the increment of the control variable at time k, that is,

$$\Delta u_N(k) = u_N(k) - u_N(k-1) \tag{9}$$

Differentiating Eq. (8) with respect to $\Delta\boldsymbol{u}_N(k)$ yields the control law

$$\boldsymbol{u}_N(k+1) = \boldsymbol{u}_N(k) - K_{N,N}\boldsymbol{y}_N(k) \tag{10}$$

where $K_{N,N} = (T_{N,N}^T Q T_{N,N} + R)^{-1} T_{N,N}^T Q$. Equation (10) is well known in the literature as the T-matrix algorithm. It can be seen from Eqs. (5) and (10) that this control algorithm introduces a discrete-time integral action, which ensures that $y_N \to 0$ as $k \to \infty$. Actually, with $Q = I_{2,2}$ and $R = 0$ deadbeat control (i.e., the output goes to zero after one discrete time step) could in principle be achieved if exact knowledge of the $T_{N,N}$ matrix were available, and if the static model, Eq. (5), were an accurate representation of rotor dynamics. However, these two assumptions are generally not satisfied, as $T_{N,N}$ can only be estimated and Eq. (5) clearly does not hold if the helicopter is not operating in steady state. Note, also, that if in the cost function, Eq. (8), one chooses $R = 0$ and Q proportional to the identity matrix, then the control law, Eq. (10), reduces to

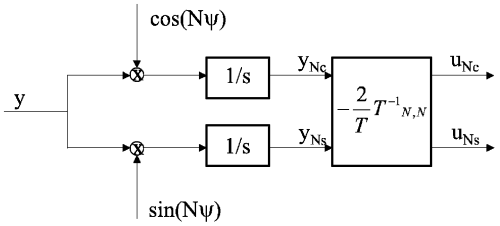

Fig. 1 Block diagram of the continuous-time SISO HHC algorithm.

$$\boldsymbol{u}_N(k+1) = \boldsymbol{u}_N(k) - T_{N,N}^{-1}\boldsymbol{y}_N(k) \tag{11}$$

which can be given a minimum variance interpretation, in the sense that this control law guarantees at each time step the closed-loop minimization of the cost function

$$J(k) = \boldsymbol{y}_N(k)^T \boldsymbol{y}_N(k) \tag{12}$$

Neglecting the effects of the sample and hold scheme of the digital implementation in the T-matrix algorithm, the overall control algorithm can be represented by the block diagram given in Figure 1.

SISO HHC with Input and Output at the Same Frequency

Following Ref. 3, choose y_{Nc} and y_{Ns} as state variables for the controller in Fig. 1. Then, the following state-space model for the HHC compensator is obtained:

$$\dot{\boldsymbol{y}}_N = A_c\boldsymbol{y}_N + B_c(\psi)\boldsymbol{y} \tag{13}$$

$$u = C_c\boldsymbol{y}_N \tag{14}$$

where

$$A_c = \begin{bmatrix} 0 & 0 \\ 0 & 0 \end{bmatrix} \tag{15}$$

$$B_c(\psi) = K_{N,N}\begin{bmatrix} \cos(N\psi) \\ \sin(N\psi) \end{bmatrix} \tag{16}$$

$$C_c = -\frac{2}{T}I_{2,2}$$

SISO HHC with Input and Output at Different Frequencies

The HHC input in the rotating system is usually not limited to the same N/rev frequency of the vibrations to be attenuated. Typically, inputs at $N-1$/rev and $N+1$/rev are also applied. (Recall that N/rev inputs of collective, longitudinal, and lateral cyclic pitch in the fixed system result in $N-1$, N, and $N+1$/rev pitch inputs in the rotating system.)

In this case, the steady-state model relating the N/rev harmonic of the output $y(t)$ to the M/rev harmonic of the pitch input $u(t)$, with $M \neq N$, can be written in the form

$$\boldsymbol{y}_N(k) = T_{N,M}\boldsymbol{u}_M(k) + \boldsymbol{y}_{0N}(k) \tag{17}$$

where $\boldsymbol{u}_M$ is defined as in Eq. (7), but for an M/rev harmonic, and where the (constant) matrix $T_{N,M}$ relates the amplitude of the M/rev control input u to the corresponding steady-state amplitude of the N/rev component of the output y. The control scheme for the attenuation of N/rev vibrations using an M/rev input can then be derived along the lines of the preceding case and is represented by the equation

$$\boldsymbol{u}_M(k+1) = \boldsymbol{u}_M(k) - K_{N,M}\boldsymbol{y}_N(k) \tag{18}$$

where $K_{N,M} = (T_{N,M}^T Q T_{N,M} + R)^{-1} T_{N,M}^T Q$. As shown in the following section, the matrix $T_{N,M}$ can be related to the harmonic

transfer function (HTF) of the controlled system, which is an extension to periodic systems of the frequency response function of a time-invariant system.[18,19] In addition, as in the case of HHC with input and output at the same frequency N/rev, the discrete control law, Eq. (18), guarantees that $y_N \to 0$ as $k \to \infty$, provided that the system can be modeled as in Eq. (17).

Similarly to the $M = N$ case, the state-space model for the case $N \neq M$ is given by

$$\dot{\boldsymbol{y}}_N = A_c \boldsymbol{y}_N + B_c(\psi)\boldsymbol{y} \tag{19}$$

$$u = C_c \boldsymbol{y}_N \tag{20}$$

where

$$A_c = \begin{bmatrix} 0 & 0 \\ 0 & 0 \end{bmatrix} \tag{21}$$

$$B_c(\psi) = K_{N,M} \begin{bmatrix} \cos(N\psi) \\ \sin(N\psi) \end{bmatrix} \tag{22}$$

$$C_c = -\frac{2}{T} I_{2,2} \tag{23}$$

This discussion shows that a coupled rotor-fuselage system with even a simple SISO HHC controller is intrinsically a system with periodic coefficients if the HHC output and the vibration to be attenuated are at two different multiples of the rotor frequency. This happens even if the rotor-fuselage system is modeled as a system with constant coefficients. Therefore, rigorous stability, performance, and robustness analyses of an HHC system can only be carried out using the tools of periodic systems theory.

MIMO with Input and Output at Arbitrary Harmonics

In typical implementations of HHC, multiharmonic signals are frequently used to attenuate several components of the vibratory loads. For example, inputs at $N-1$/, N/, and $N+1$/rev, sine and cosine (for a total of six inputs), could be used simultaneously to control six components of the N/rev vibratory hub forces and moments. Therefore, this section extends the preceding SISO discussion to a MIMO HHC system. We will consider a general configuration in which output measurements of N/rev vibration are available at n different locations, while a number m of harmonics at frequencies N_i, $i = 1, \ldots, m$ are applied on the control input $\boldsymbol{u}$. In this case, the measurement vector has $2n$ elements and is defined as

$$\boldsymbol{y}_N^T = \begin{bmatrix} y_{\mathrm{Nc}}^1 & \cdots & y_{\mathrm{Nc}}^n & \cdots & y_{\mathrm{Ns}}^1 & \cdots & y_{\mathrm{Ns}}^n \end{bmatrix} \tag{24}$$

where y_{Nc}^i and y_{Ns}^i, $i = 1, \ldots, n$ are, respectively, the cosine and sine components of the ith N/rev output, which can be, for example, a force or moment component, or a component of a linear or angular acceleration at one or more points of the fuselage.

The HHC input vector $\boldsymbol{u}$ has $2m$ elements and is defined as

$$\boldsymbol{u}^T = \begin{bmatrix} u_{N_1 c} & u_{N_1 s} \cdots u_{N_2 c} & u_{N_2 s} \cdots u_{N_m c} & u_{N_m s} \end{bmatrix} \tag{25}$$

where $u_{N_i c}$, $i = 1, \ldots, m$ and $u_{N_i s}$, $i = 1, \ldots, m$ are the cosine and sine component of the HHC input, at desired harmonics not necessarily equal to N/rev.

Assume now, as in the SISO case, that input and output harmonics are related by the linear equation

$$\boldsymbol{y}_N(k) = T\boldsymbol{u}(k) + \boldsymbol{y}_{0N}(k) \tag{26}$$

where T is a $2n \times 2m$ constant coefficient matrix, which is again related to the HTF of the time-periodic linearized model of the helicopter. Then, the T-matrix algorithm is given by

$$\boldsymbol{u}(k+1) = \boldsymbol{u}(k) - K\boldsymbol{y}_N(k) \tag{27}$$

where $K = (T^T Q T + R)^{-1} T^T Q$, where $Q = Q^T \geq 0$ and $R = R^T > 0$ are cost-weighting matrices of suitable dimensions.

In the MIMO case, the operation of the HHC control law differs considerably depending on the relationship between the number of control inputs and measured variables that are available. To illustrate this difference, the formulation of the T-matrix algorithm in the MIMO case with $Q = I_{n,n}$ and $R = 0$ will be presented separately for the cases of $n = m$ and of $n > m$. (The case $n < m$, that is, with more controls than vibration outputs to be attenuated, is not likely to be important in practice.)

In the case of a "square" control problem, that is, when $n = m$, the SISO algorithm can be readily extended to

$$\boldsymbol{u}(k+1) = \boldsymbol{u}(k) - T^{-1}\boldsymbol{y}_N(k) \tag{28}$$

On the other hand, if $n > m$ the matrix T is no longer square, and the discrete-time control algorithm must be written as

$$\boldsymbol{u}(k+1) = \boldsymbol{u}(k) - T^{\dagger}\boldsymbol{y}_N(k) \tag{29}$$

where $T^{\dagger} = (T^T T)^{-1} T^T$ is the pseudoinverse of T. In particular, the minimum of the cost function equals zero only in the $n = m$ case, that is, unless one considers (at least) the square case, it is not possible to guarantee that the vibratory disturbance will be zeroed on all output channels.

The equivalent continuous-time formulation for the MIMO HHC compensator, described in discrete form by Eq. (27), can be obtained by applying the already described SISO results. Therefore, considering first the case of a control system with as many inputs as outputs, the state-space formulation is given by the order $2n$ system:

$$\dot{\boldsymbol{y}}_N = A_c \boldsymbol{y}_N + B_c(\psi)\boldsymbol{y} \tag{30}$$

$$u = C_c \boldsymbol{y}_N \tag{31}$$

where A_c is the $2n \times 2n$ matrix

$$A_c = \begin{bmatrix} 0 & 0 & \cdots & 0 \\ 0 & 0 & \cdots & 0 \\ \vdots & \vdots & & \vdots \\ 0 & 0 & \cdots & 0 \end{bmatrix} \tag{32}$$

$B_c(\psi)$ is the $2n \times n$ matrix

$$B_c(\psi) = K \begin{bmatrix} \cos(N\psi) I_{n,n} \\ \sin(N\psi) I_{n,n} \end{bmatrix} \tag{33}$$

$$C_c = -\frac{2}{T} I_{2n \times 2n} \tag{34}$$

For example, consider the case of a control system relying on the application of $N-1$/, N/, and $N+1$/rev inputs in the rotating frame to attenuate one component of the accelerations in $n = 3$ different locations in the fuselage, so that $m = 3$, $N_1 = N-1$, $N_2 = N$, and $N_3 = N+1$ and

$$u^T = [\theta_{(N-1)c} \theta_{(N-1)s} \quad \theta_{\mathrm{Nc}} \theta_{\mathrm{Ns}} \quad \theta_{(N+1)c} \theta_{(N+1)s}] \tag{35}$$

$$y^T = [y_1 \quad y_2 \quad y_3] \tag{36}$$

Then, the state-space model for the controller is given by

$$A_c = 0_{6\times 6} \tag{37}$$

$$B_c(\psi) = K \begin{bmatrix} \cos(N\psi) & 0 & 0 \\ 0 & \cos(N\psi) & 0 \\ 0 & 0 & \cos(N\psi) \\ \sin(N\psi) & 0 & 0 \\ 0 & \sin(N\psi) & 0 \\ 0 & 0 & \sin(N\psi) \end{bmatrix} \tag{38}$$

As in the SISO case, because the control inputs are directly given by the higher harmonics of θ, there is no need for a "modulation" term in matrix C_c, which therefore turns out to be constant:

$$C_c = -(2/T)I_{6\times 6} \tag{39}$$

Similar expressions can be worked out in the case of a control system with more outputs than inputs.

Definition of the T Matrix in Terms of the Helicopter Models

The control laws discussed in the preceding section call for the availability of input/output models for the helicopter response to higher-harmonic-control inputs. This section provides some background on the frequency response of time-periodic systems and uses such analytical tools to derive explicit expressions for the T matrix.

Development of the Harmonic Transfer Function

This section summarizes the main aspects of the development of the HTF.[18] Consider a continuous-time linear periodic system:

$$\dot{\boldsymbol{x}}(t) = A(t)\boldsymbol{x}(t) + B(t)\boldsymbol{u}(t), \qquad \boldsymbol{y}(t) = C(t)\boldsymbol{x}(t) + D(t)\boldsymbol{u}(t) \tag{40}$$

Each matrix can be expanded in a complex Fourier series

$$A(t) = \sum_{m=-\infty}^{\infty} A_m e^{jm\Omega t} \tag{41}$$

and similarly for $B(t)$, $C(t)$, and $D(t)$. The system can be analyzed in the frequency domain as follows. Introduce the class of exponentially modulated periodic (EMP) signals.[18] The (complex) signal $u(t)$ is said to be EMP of period T and modulation s if

$$u(t) = \sum_{k=-\infty}^{\infty} u_k e^{s_k t} = e^{st} \sum_{k=-\infty}^{\infty} u_k e^{jk\Omega t} \tag{42}$$

where $t \geq 0$, $s_k = s + jk\Omega$, and s is a complex scalar.

The class of EMP signals is a generalization of the class of T-periodic signals, that is, of signals with period T: in fact, an EMP signal with $s = 0$ is just an ordinary time-periodic signal.

In much the same way as a time-invariant system subject to a (complex) exponential input has an exponential steady-state response, a periodic system subject to an EMP input has an EMP steady-state response. In such a response, all signals of interest (x, $\dot{x}$, y) can be expanded as EMP signals. By deriving Fourier expansions for $A(t)$, $B(t)$, $C(t)$, and $D(t)$, it is possible to prove that the EMP steady-state response of the system can be expressed as the infinite dimensional matrix equation with constant elements[18]

$$s\boldsymbol{\mathcal{X}} = (\mathcal{A} - \mathcal{N})\boldsymbol{\mathcal{X}} + \mathcal{B}\boldsymbol{\mathcal{U}}, \qquad \boldsymbol{\mathcal{Y}} = \mathcal{C}\boldsymbol{\mathcal{X}} + \mathcal{D}\boldsymbol{\mathcal{U}} \tag{43}$$

where $\boldsymbol{\mathcal{X}}$, $\boldsymbol{\mathcal{U}}$, and $\boldsymbol{\mathcal{Y}}$ are doubly infinite vectors formed with the harmonics of $\boldsymbol{x}$, $\boldsymbol{u}$, and $\boldsymbol{y}$ respectively, organized in the following fashion:

$$\boldsymbol{\mathcal{X}}^T = \begin{bmatrix} \cdots & \boldsymbol{x}_{-2}^T & \boldsymbol{x}_{-1}^T & \boldsymbol{x}_0^T & \boldsymbol{x}_1^T & \boldsymbol{x}_2^T & \cdots \end{bmatrix} \tag{44}$$

and similarly for $\boldsymbol{\mathcal{U}}$ and $\boldsymbol{\mathcal{Y}}$. $\mathcal{A}, \mathcal{B}, \mathcal{C}$, and $\mathcal{D}$ are doubly infinite Toeplitz matrices formed with the harmonics of $A(\cdot)$, $B(\cdot)$, $C(\cdot)$, and $D(\cdot)$, respectively, as follows:

$$\mathcal{A} = \begin{bmatrix} \ddots & \vdots & \vdots & \vdots & \vdots & \vdots & \\ \cdots & A_0 & A_{-1} & A_{-2} & A_{-3} & A_{-4} & \cdots \\ \cdots & A_1 & A_0 & A_{-1} & A_{-2} & A_{-3} & \cdots \\ \cdots & A_2 & A_1 & A_0 & A_{-1} & A_{-2} & \cdots \\ \cdots & A_3 & A_2 & A_1 & A_0 & A_{-1} & \cdots \\ \cdots & A_4 & A_3 & A_2 & A_1 & A_0 & \cdots \\ & \vdots & \vdots & \vdots & \vdots & \vdots & \ddots \end{bmatrix} \tag{45}$$

(and similarly for $\mathcal{B}, \mathcal{C}$, and $\mathcal{D}$), where the submatrices A_n in Eq. (45) are the coefficients of the Fourier expansion of matrix $A(t)$, given in Eq. (41). To relate these coefficients to those of the Fourier-series expansion in trigonometric form, Eq. (1), recall that the Fourier-series expansion of a scalar function can be rewritten in complex exponential form, that is,

$$a(t) = a_0 + \sum_{k=1}^{\infty} (a_{\mathrm{nc}} \cos n\omega t + a_{\mathrm{ns}} \sin n\omega t) = \sum_{k=-\infty}^{\infty} a_k e^{jk\omega t}$$

with $a_k = (a_{\mathrm{kc}} - ja_{\mathrm{ks}})/2$ and $a_{-k} = (a_{\mathrm{kc}} + ja_{\mathrm{ks}})/2$, $k = 1, 2, \ldots$. Therefore, the coefficients of Eqs. (41) and (1) are related by

$$A_k = \tfrac{1}{2}(A_{\mathrm{kc}} - jA_{\mathrm{ks}})$$

$$A_{-k} = \tfrac{1}{2}(A_{\mathrm{kc}} + jA_{\mathrm{ks}}) \qquad k = 1, 2, \ldots \tag{46}$$

with A_0 identical in both Eqs. (41) and (1). Similar relations hold for the harmonics of B, C, and D.

Matrix $\mathcal{N}$ is a block-diagonal complex-valued matrix given by

$$\mathcal{N} = \mathrm{blkdiag}\{jn\Omega I\} = j\Omega \begin{bmatrix} \ddots & \vdots & \vdots & \vdots & \vdots & \vdots & \\ \cdots & -2I & 0 & 0 & 0 & 0 & \cdots \\ \cdots & 0 & -I & 0 & 0 & 0 & \cdots \\ \cdots & 0 & 0 & 0 & 0 & 0 & \cdots \\ \cdots & 0 & 0 & 0 & I & 0 & \cdots \\ \cdots & 0 & 0 & 0 & 0 & 2I & \cdots \\ & \vdots & \vdots & \vdots & \vdots & \vdots & \ddots \end{bmatrix} \tag{47}$$

where I is the identity matrix of size equal to the number of states.

From Eq. (43), one can define the HTF $\mathcal{G}(s)$ as the operator:

$$\mathcal{G}(s) \stackrel{def}{=} \mathcal{C}[s\mathcal{I} - (\mathcal{A} - \mathcal{N})]^{-1}\mathcal{B} + \mathcal{D} \tag{48}$$

which relates the input harmonics and the output harmonics (contained in the infinite vectors $\boldsymbol{\mathcal{U}}$ and $\boldsymbol{\mathcal{Y}}$, respectively). Equation (48) is the extension to the case of periodic systems of the corresponding constant coefficient expression for the transfer function

$$G(s) = C[sI - A]^{-1}B + D \tag{49}$$

In particular, if $s = 0$, which, in the helicopter case, corresponds to the steady-state response of the system to a periodic input of basic frequency N/rev, the appropriate input/output operator for periodic systems becomes

$$\mathcal{G}(0) = \mathcal{C}[\mathcal{N} - \mathcal{A}]^{-1}\mathcal{B} + \mathcal{D} \tag{50}$$

Definition of the T Matrix

The $T_{N,N}$, $T_{N,M}$, and T matrices used in the formulation of the HHC and PHHC algorithms can be related to the elements of the HTF of the linearized helicopter model, as follows.

First of all, note that according to the definition of the control input vector $\boldsymbol{u}$, which has been adopted, the rotor will be subject to a proper, steady-state higher-harmonic-control input whenever the control vector $\boldsymbol{u}$ is constant. This implies that to define the T matrix for the helicopter we only have to study the response of the periodic helicopter models to an EMP input with $s = 0$, that is, we only have to compute the input/output operator $\hat{\mathcal{G}}(0)$. For example, consider the linear time-periodic system, Eq. (40), and the constant input $\boldsymbol{u}(t) = \boldsymbol{u}_0$. The vector $\boldsymbol{\mathcal{U}}$ corresponding to $\boldsymbol{u}(t) = \boldsymbol{u}_0$ is given by

$$\boldsymbol{\mathcal{U}}^T = \begin{bmatrix} \cdots & 0 & 0 & \boldsymbol{u}_0^T & 0 & 0 & \cdots \end{bmatrix} \tag{51}$$

and the steady-state response $\boldsymbol{\mathcal{Y}}$ of the periodic system is given by

$$\boldsymbol{\mathcal{Y}} = \mathcal{G}(0)\boldsymbol{\mathcal{U}} \tag{52}$$

which can be equivalently written as

$$\begin{bmatrix} \vdots \\ y_{-2N} \\ y_{-N} \\ y_0 \\ y_N \\ y_{2N} \\ \vdots \end{bmatrix} = \begin{bmatrix} \ddots & \vdots & \vdots & \vdots & \vdots & \vdots & \\ \cdots & G_{-2N,-2N} & G_{-2N,-N} & G_{-2N,0} & G_{-2N,N} & G_{-2N,2N} & \cdots \\ \cdots & G_{-N,-2N} & G_{-N,-N} & G_{-N,0} & G_{-N,N} & G_{-N,2N} & \cdots \\ \cdots & G_{0,-2N} & G_{0,-N} & G_{0,0} & G_{0,N} & G_{0,2N} & \cdots \\ \cdots & G_{N,-2N} & G_{N,-N} & G_{N,0} & G_{N,N} & G_{N,2N} & \cdots \\ \cdots & G_{2N,-2N} & G_{2N,-N} & G_{2N,0} & G_{2N,N} & G_{2N,2N} & \cdots \\ \ddots & \vdots & \vdots & \vdots & \vdots & \vdots & \ddots \end{bmatrix} \times \begin{bmatrix} \vdots \\ 0 \\ 0 \\ u_0 \\ 0 \\ 0 \\ \vdots \end{bmatrix} \tag{53}$$

From Eq. (53) we have that

$$\begin{bmatrix} y_{-N} \\ y_N \end{bmatrix} = \begin{bmatrix} G_{-N,0} \\ G_{N,0} \end{bmatrix} u_0 \tag{54}$$

and converting the N/rev harmonics of the output from exponential to trigonometric form we have that

$$\begin{bmatrix} y_{\mathrm{Nc}} \\ y_{\mathrm{Ns}} \end{bmatrix} = 2 \begin{bmatrix} \mathrm{Real}\,[G_{N,0}] \\ \mathrm{Imag}\,[G_{N,0}] \end{bmatrix} u_0 \tag{55}$$

(note that $G_{-N,0}$ and $G_{N,0}$ are complex conjugate) so that the T matrix is given by

$$T = 2 \begin{bmatrix} \mathrm{Real}\,[G_{N,0}] \\ \mathrm{Imag}\,[G_{N,0}] \end{bmatrix} \tag{56}$$

Construction of the T Matrix

From a practical point of view, the preceding theoretical analysis of the frequency response of periodic system and the corresponding definitions for the T matrix relating selected input-output frequencies only rely on the use of infinite dimensional matrices. When it comes to the numerical construction of the T matrix, however, one has to resort to finite dimensional approximations of the system matrices $\mathcal{A}$, $\mathcal{B}$, $\mathcal{C}$, and $\mathcal{D}$. Consider, for example, the problem of constructing the T matrix, as defined in Eq. (56) for a periodic system of the form of Eq. (40) with n outputs, m inputs, and n_s states. First of all, one chooses the dimension of the expansions $\mathcal{A}$, $\mathcal{B}$, $\mathcal{C}$, and $\mathcal{D}$ for the state-space matrices A, B, C, and D, in terms of the number of block rows one wants to take into account in $\mathcal{A}$. For example, if we choose to include a number $n_B = 5$ of blocks in each row of the expansion of the system matrices, then $\mathcal{A}$ has dimension $n_s n_B \times n_s n_B$ and is given by

$$\mathcal{A} = \begin{bmatrix} A_0 & A_{-1} & A_{-2} & A_{-3} & A_{-4} \\ A_1 & A_0 & A_{-1} & A_{-2} & A_{-3} \\ A_2 & A_1 & A_0 & A_{-1} & A_{-2} \\ A_3 & A_2 & A_1 & A_0 & A_{-1} \\ A_4 & A_3 & A_2 & A_1 & A_0 \end{bmatrix} \tag{57}$$

and similarly for $\mathcal{B}$, $\mathcal{C}$, and $\mathcal{D}$. Therefore, the HTF is given by the $2nn_B \times mn_B$ matrix, as follows:

$$\begin{bmatrix} y_{-2N} \\ y_{-N} \\ y_0 \\ y_N \\ y_{2N} \end{bmatrix} = \mathcal{G}(0)\,\mathcal{U}$$

$$= \begin{bmatrix} G_{-2N,-2N} & G_{-2N,-N} & G_{-2N,0} & G_{-2N,N} & G_{-2N,2N} \\ G_{-N,-2N} & G_{-N,-N} & G_{-N,0} & G_{-N,N} & G_{-N,2N} \\ G_{0,-2N} & G_{0,-N} & G_{0,0} & G_{0,N} & G_{0,2N} \\ G_{N,-2N} & G_{N,-N} & G_{N,0} & G_{N,N} & G_{N,2N} \\ G_{2N,-2N} & G_{2N,-N} & G_{2N,0} & G_{2N,N} & G_{2N,2N} \end{bmatrix} \begin{bmatrix} 0 \\ 0 \\ u_0 \\ 0 \\ 0 \end{bmatrix} \tag{58}$$

The blocks $G_{-N,0}$, $G_{N,0}$ can be extracted from $\mathcal{G}(0)$ as the submatrices $\mathcal{G}_{ij}(0)$, $i = 2n+1, \ldots, 3n$ and $j = 2m+1, \ldots, 3m$, and $\mathcal{G}_{ij}(0)$, $i = 4n+1, \ldots, 5n$ and $j = 2m+1, \ldots, 3m$, respectively. Clearly, the choice of the number of block rows n_B will affect the accuracy of the numerical construction (see Ref. 20 for an analysis of the effect of truncation in the study of frequency response operators), so as a general rule n_B should be chosen sufficiently large to ensure that the T matrix constructed from the truncated HTF gives a good approximation to the actual T matrix.

Formulation of the Coupled Helicopter/HHC Model

The compensator will be designed along the lines of Ref. 18. Denote with $A(\psi)$, $B(\psi)$, $C(\psi)$, and $D(\psi)$ the matrices for the linear time periodic (LTP) state-space model of the helicopter, for the selected input/output pair. Similarly, denote with $A_c(\psi)$, $B_c(\psi)$, $C_c(\psi)$ the compensator's state-space model. Then the closed-loop LTP state matrix $A_e(\psi)$ is given by

$$A_e(\psi) = \begin{bmatrix} A(\psi) & B(\psi)C_c(\psi) \\ B_c(\psi)C(\psi) & A_c(\psi) + B_c(\psi)D(\psi)C_c(\psi) \end{bmatrix} \tag{59}$$

The closed-loop stability of the helicopter with HHC is then given by the characteristic exponents of $A_e(\psi)$ and will be studied as a function of the design parameters Q and R.

Results

This section presents closed-loop stability and response results for a coupled helicopter-HHC system. The stability results are obtained from the linearized model of Eq. (59) or its constant coefficient approximation. The closed-loop response results are obtained from the full nonlinear simulation of the coupled helicopter-HHC system. The primary meaning of the words closed loop is that the HHC vibration control loops are closed. Although a small amount of feedback was added to the model to stabilize the flight dynamic modes, the flight control system model is not realistic enough to enable reliable studies of HHC-flight control system interaction.

The helicopter configuration used for the present study is similar to the Eurocopter B0-105, with a thrust coefficient $C_T/\sigma = 0.071$. Three blade modes are used in the modal coordinate transformation, namely, the fundamental flap, lag, and torsion modes, with natural frequencies of 1.12/rev, 0.7/rev, and 3.4/rev, respectively. Because the aerodynamic model consists of a simple linear inflow with quasi-steady aerodynamics, and because fuselage flexibility has been neglected, vibratory loads and c.g. accelerations, and consequently

also HHC inputs, tend to be underestimated. Therefore, their absolute values can be considered representative only in a qualitative sense. However, the overall simulation model is likely reasonable for stability studies and for a general assessment of the design and closed-loop analysis methodology.

For all of the vibratory response results, the helicopter is first trimmed in steady, straight flight at the desired velocity with the HHC system turned off. Then, the nonlinear simulation begins with the pilot controls held fixed at their trim values and the HHC system turned on at time $t = 0$. The Q and R matrices in Eq. (8) have been defined as $Q = I_{6,6}$ and $R = rI_{6,6}$, respectively, where $I_{6,6}$ is an identity matrix with six rows and columns, and r is a parameter that varies from $r = 0$ (no restriction on control effort) to $r = 1000$.

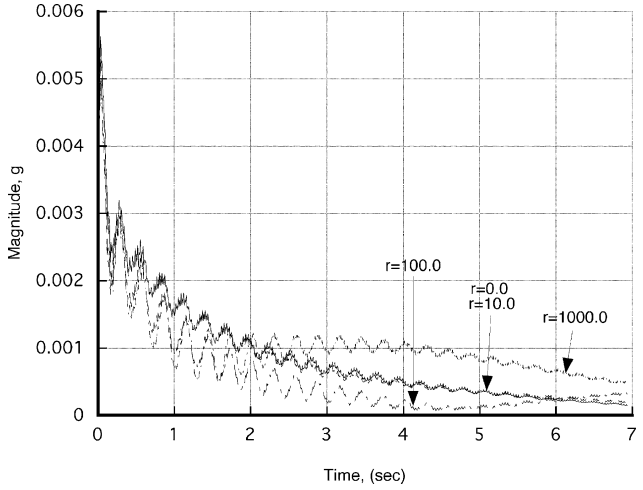

Fig. 2 Peak-to-peak 4/rev vertical accelerations at the helicopter center of mass for $V = 80$ kn ($\mu = 0.188$).

Results for $V = 80$ kn

Figure 2 shows the peak-to-peak magnitude of the 4/rev component of the vertical (i.e., along the z-body axis) acceleration at the c.g., for a speed $V = 80$ kn, corresponding to $\mu = 0.19$. The figure shows four curves, one each for values of $r = 0$, 10, 100, and 1000, corresponding to increasing restrictions on the control effort. The high-frequency oscillations visible in the curves of this, and of many subsequent figures, are largely an artifact of the numerical procedure used to extract the 4/rev magnitude and phase from the time histories of the accelerations. Clearly, the HHC system is very effective and reduces the 4/rev vertical acceleration to a small fraction of its trim value in just a few seconds. The vibration attenuation is also very clear for the c.g. roll acceleration $\dot{p}$ and pitch acceleration $\dot{q}$: the magnitudes of the 4/rev components are shown in Fig. 3. Both $\dot{p}$ and $\dot{q}$ are reduced to 5% or less of their trim values in no more than 6–7 s.

Figure 4 shows the magnitude of the 3/, 4/, and 5/rev components of the HHC input for the cases $r = 0$ and 1000. Figure 5 shows the corresponding phase angles. Comparing the two sets of results, it can be seen that the controls reach their steady-state values much more quickly for the case $r = 0$ than for $r = 1000$. In the latter case, the steady-state values of θ_3 and θ_5 have not yet been reached at the end of 7 s of simulation.

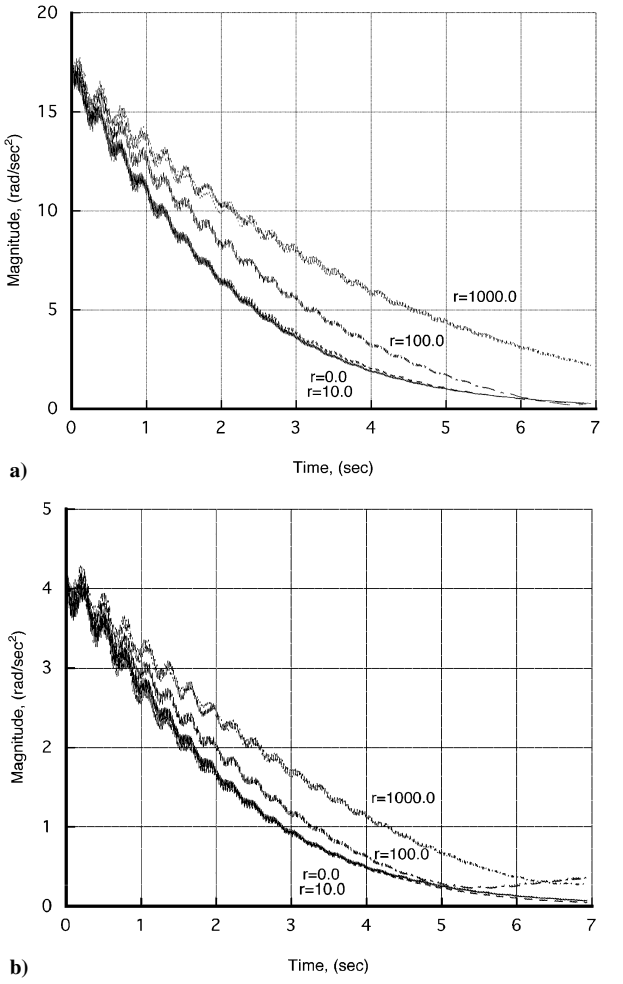

Fig. 3 Peak-to-peak 4/rev a) roll and b) pitch accelerations at the helicopter center of mass for $V = 80$ kn ($\mu = 0.188$).

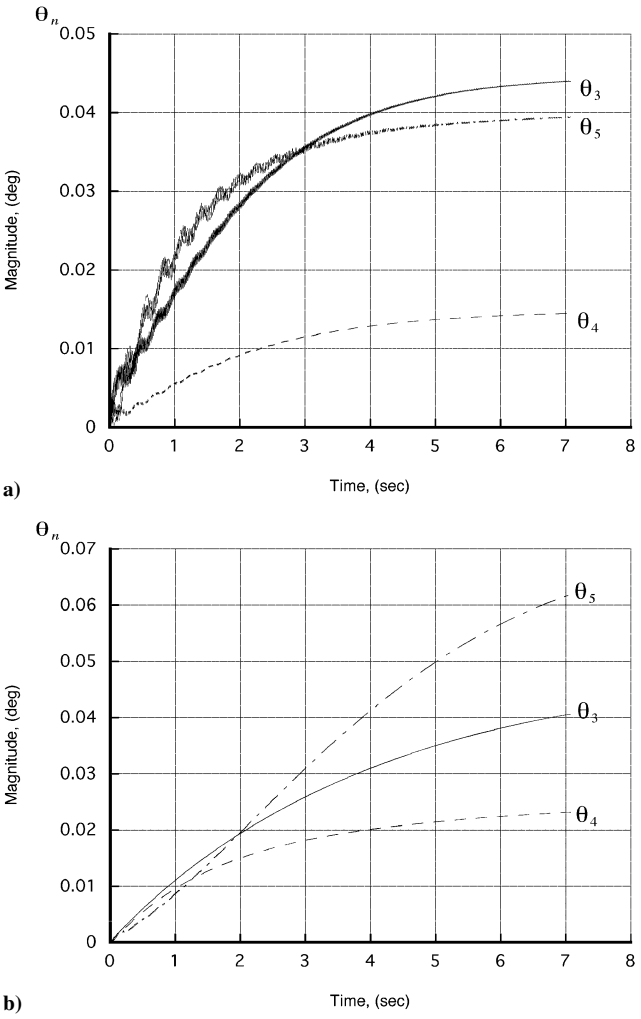

Fig. 4 HHC input amplitude in degrees for $V = 80$ kn ($\mu \approx 0.189$) for a) $r = 0$ and b) $r = 1000$.

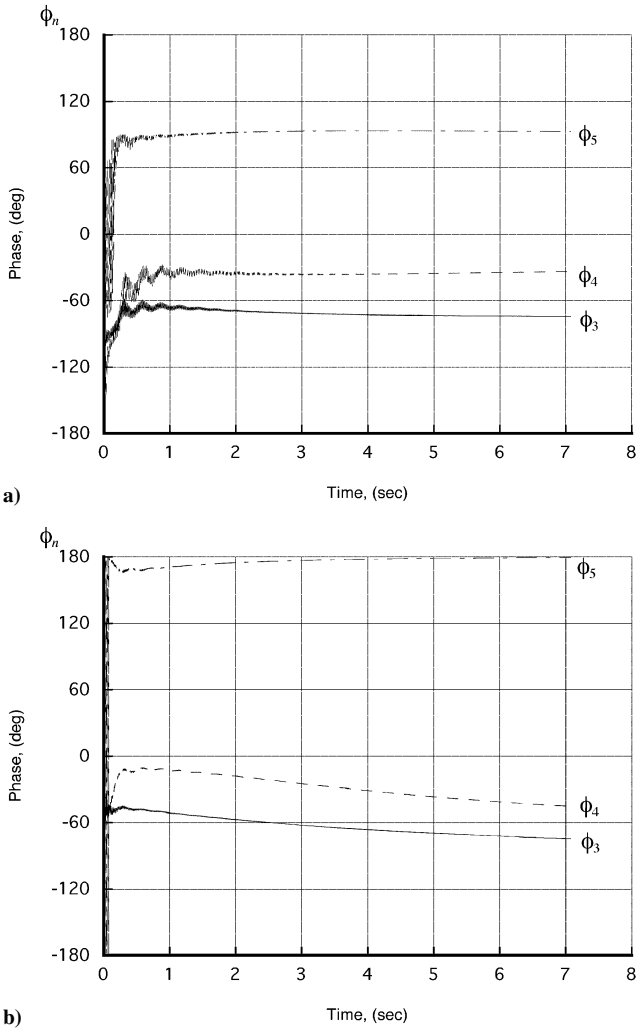

Fig. 5 HHC input phase in degrees for $V = 80$ kn ($\mu \approx 0.189$) for a) $r = 0$ and b) $r = 1000$.

The action of the HHC system, and the consequent vibration reduction, occurs within times of the order of 5–7 s or, equivalently, of about 1 rad/s. These are also typical timescales for flight control systems and also overlap typical piloting frequencies. Therefore, the results shown earlier indicate the possibility of interaction with the stability and control characteristics of the helicopter.

It is also interesting to consider the closed-loop eigenvalues of the system. The computation of the closed-loop state matrix A_e, Eq. (59), was carried out by linearizing the augmented nonlinear set of equations. Figure 6 shows a root-locus plot of just the controller eigenvalues for increasing values of r, using a constant coefficient approximation to A_e. The system displays a mildly unstable complex conjugate pair at 80 kn, but there is no trace of the instability in the closed-loop simulations using the full nonlinear system, already shown. The instability is probably caused by the errors made in modeling the periodic system with a constant coefficient approximation. In fact, when the periodicity is fully taken into account, the instability disappears. This can be seen in Fig. 7, which shows the real parts of both the stability eigenvalues of the linear time invariant (LTI) system and the Floquet characteristic exponents of the LTP system, for the least damped modes. None of the characteristic exponents, which include controller, rotor, and rigid-body modes, becomes unstable for any of the values of r considered. This confirms that, whenever the HHC input includes harmonics that are different from the harmonic that one is trying to attenuate, the closed-loop problem is intrinsically time periodic. Constant coefficient approximations might not yield correct closed-loop stability results, as in this case, even at lower advance ratios, where constant coefficient

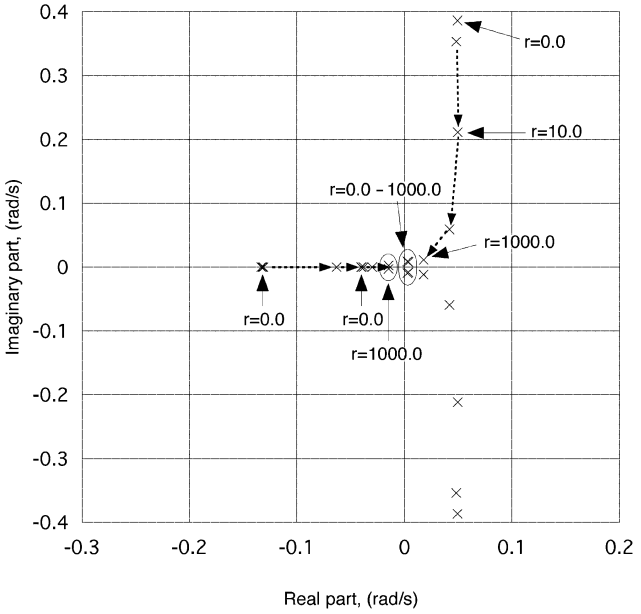

Fig. 6 Root locus of controller eigenvalues of LTI closed-loop system for $V = 80$ kn.

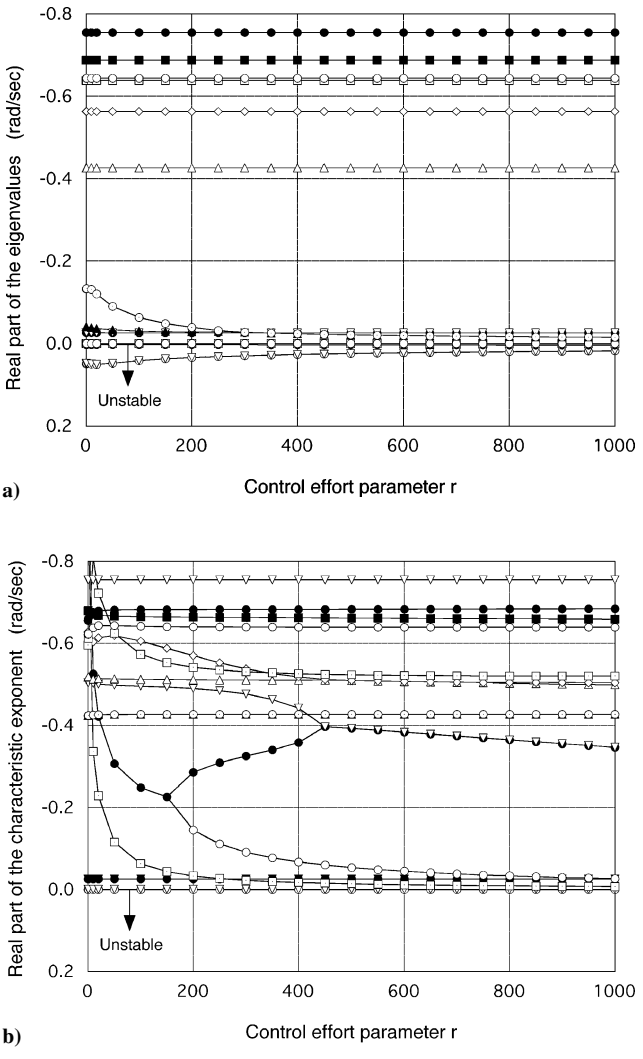

Fig. 7 Real parts of a) eigenvalues and b) characteristic exponents of the least damped modes, $V = 80$ kn.

approximations give acceptable results for the open-loop system. Apart from the heading eigenvalue at the origin, the modes with the lowest amount of damping are those of the controller.

Finally, the position of the eigenvalues appears to be linked to the vibration reduction performance. In general, for the highest control effort (tuning parameter $r = 0$) controller eigenvalues tend to be farther away from the origin, and as r increases they come closer to it.

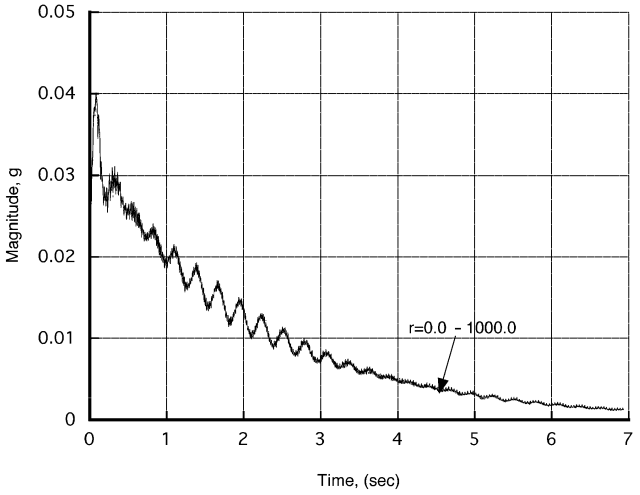

Fig. 8 Peak-to-peak 4/rev vertical accelerations at the helicopter center of mass for $V = 140$ kn ($\mu = 0.330$).

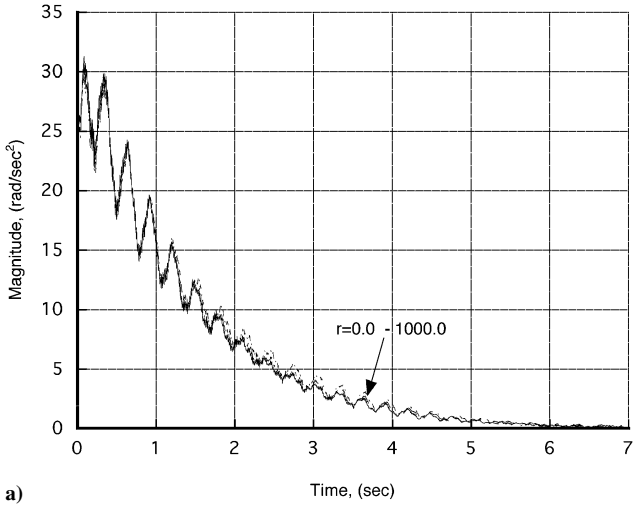

a)

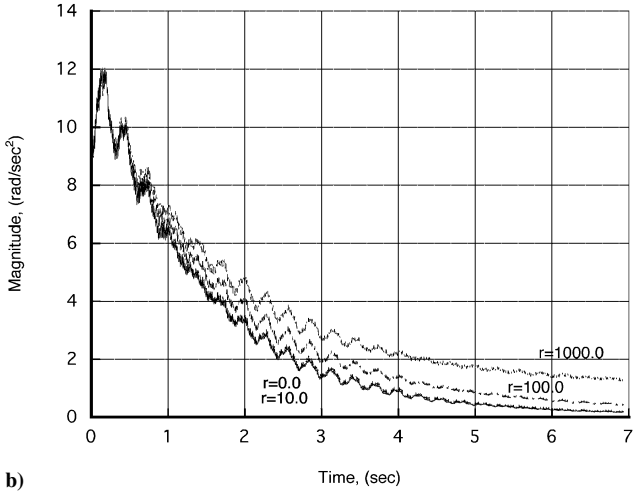

b)

Fig. 9 Peak-to-peak 4/rev a) roll and b) pitch accelerations at the helicopter center of mass for $V = 140$ kn ($\mu = 0.330$).

Results for $V = 140$ and 170 kn

Figures 8 and 9 show the 4/rev c.g. acceleration components at a speed of $V = 140$ kn, corresponding to an advance ratio $\mu = 0.33$. The magnitude of the vertical acceleration is shown in Fig. 8. The HHC is extremely effective and reduces the magnitude of the 4/rev accelerations to almost zero within about 7 s. Near-perfect attenuation of the roll acceleration $\dot{p}$ can be seen in Fig. 9. The figure also shows that the pitch acceleration $\dot{q}$ is also very well attenuated by the HHC system.

The magnitudes of the corresponding values of the 3/, 4/, and 5/rev inputs are shown in Fig. 10 for the cases $r = 0$ and 1000. The steady-state values of each control are reached in about 7 s; therefore, the timescale of action of the controller is approximately the same as in the 80-kn case. Differently from the 80-kn case, the control time histories for $r = 0$ and 1000 are very similar. A possible reason for this is that the numerical "size" of the T matrix increases significantly as a function of airspeed: this makes the controller gain less and less sensitive to changes in r.

The LTI, closed-loop eigenvalues for $V = 140$ kn are shown in Fig. 11. At this speed, all of the eigenvalues are stable, with the partial exception of a complex controller eigenvalue, which is unstable but extremely close to the origin. The real parts of both the stability eigenvalues of the LTI system and the Floquet characteristic exponents of the LTP system, for the least damped modes, are shown in Fig. 12. All of the characteristic exponents are stable. As in the $V = 80$ kn case, the modes with the lowest amount of damping are those of the controller.

Finally, Fig. 13 shows one result for the case $V = 170$ kn, corresponding to $\mu = 0.4$. Note that the simulation cannot determine a trim state at this speed. Therefore, the drag of the fuselage was

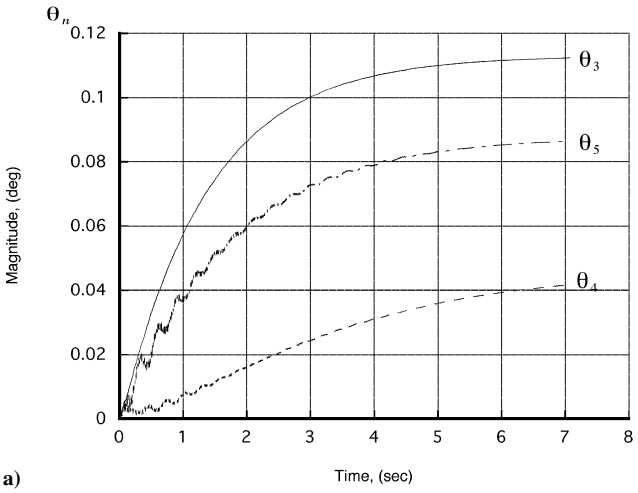

a)

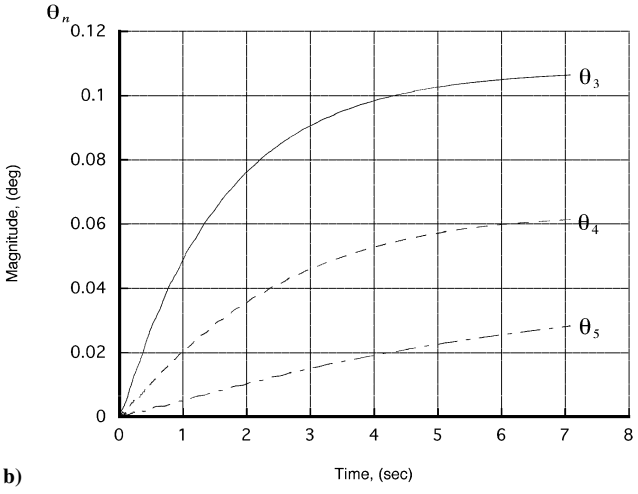

b)

Fig. 10 HHC input amplitude in degrees for $V = 140$ kn ($\mu \approx 0.33$) for a) $r = 0$ and b) $r = 1000$.

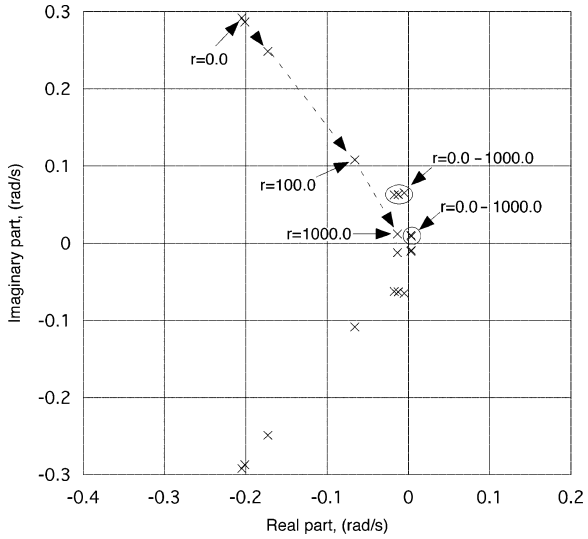

Fig. 11 Root locus of controller eigenvalues of LTI closed-loop system for $V = 140$ kn.

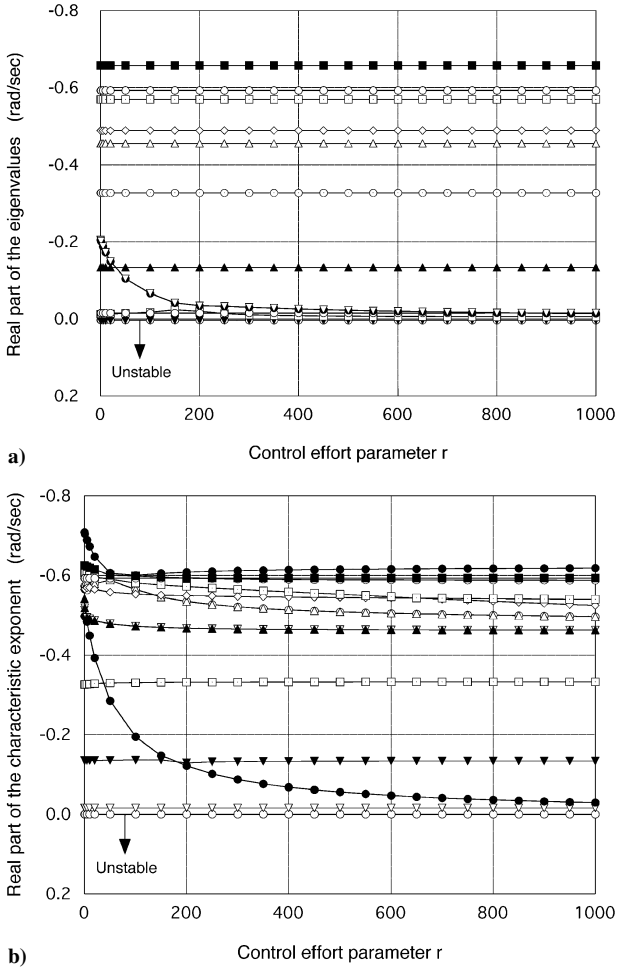

Fig. 12 Real parts of a) eigenvalues and b) characteristic exponents of the least damped modes for $V = 140$ kn.

arbitrarily reduced until a trimmed state could be achieved. Figure 13 shows baseline and HHC-on magnitudes of the 4/rev component of the vertical acceleration. Again, the HHC is very effective at attenuating vibrations, and the attenuation occurs on the same timescales as for the speeds already shown. Additional results were obtained for this speed, but are not presented here for reasons of space. However, the overall trends are the same as seen for the $V = 80$ and 140 kn cases, except that the closed-loop LTI system is stable.

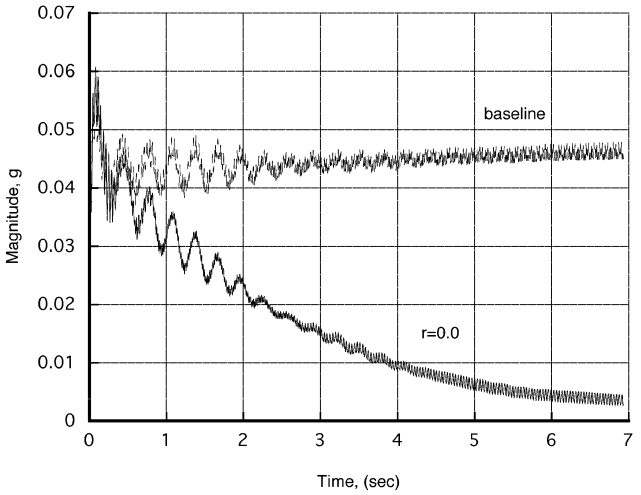

Fig. 13 Peak-to-peak 4/rev vertical accelerations at the helicopter center of mass for $V = 170$ kn ($\mu = 0.4$); reduced fuselage drag.

Conclusions

The paper presented the development of a state-space formulation for a multi-input/multi-output (MIMO) higher-harmonic-control (HHC) system. The development started with a simple state-space derivation for the continuous-time form of a single-input/single-output HHC compensator with input and output at the same rotor harmonic; then the same approach was extended to the case of different harmonics in input and output, which resulted in a periodic single-input/single-output HHC compensator; finally, that result was generalized for the derivation of the state-space form for a MIMO HHC controller. The paper also presented results of a numerical investigation into the performance and stability properties of a closed-loop HHC system, implemented in the rotating system, based on a simulation study of the coupled rotor-fuselage dynamics of a four-bladed hingeless rotor helicopter.

The results of the simulation study indicate the following:

1) The HHC controller is very effective in reducing the desired components of the 4/rev accelerations at the center of gravity. The percentage reductions indicated by the simulations are in excess of 80–90%. However, because the simplifications in the model lead to underestimating these vibratory components the absolute values of the reduction and of the control inputs might not be fully reliable.

2) The vibration attenuation occurs within 5–7 s after the HHC system is turned on. This is equivalent to a frequency of around 1 rad/s, which is within the frequency band in which flight control systems and human pilots tend to operate. Therefore, the interactions and potential adverse effects on the stability and control characteristics of the helicopter should be explored.

3) The HHC problem is intrinsically time periodic if the HHC inputs include frequencies other than the frequency one wishes to attenuate. This is true even if the rest of the model is assumed to be time invariant. In these cases, the closed-loop stability results obtained using a constant coefficient approximations might be incorrect even at lower values of the advance ratio μ, where constant coefficient approximation of the open-loop dynamics is accurate.

Acknowledgments

This research was supported by the U. S. Army Research Office, under the Grant 41569-EG, Technical Monitor Gary Anderson. This paper was presented at the 29th European Rotorcraft Forum, Friedrichshafen, Germany, 16–18 September 2003.

References

[1]Friedmann, P. P., and Millott, T., "Vibration Reduction in Rotorcraft Using Active Control-A Comparison of Various Approaches," *Journal of Guidance, Control, and Dynamics*, Vol. 18, No. 4, 1995, pp. 664–673.

[2]Teves, D., Niesl, G., Blaas, A., and Jacklin, S., "The Role of Active Control in Future Rotorcraft," Paper III.10.1-17, *Proceedings of the 21st European Rotorcraft Forum*, Aug. 1995.

[3]Wereley, N., and Hall, S., "Linear Control Issues in the Higher Harmonic Control of Helicopter Vibrations," *Proceedings of the 45th Forum of the American Helicopter Society*, Alexandria, VA, 1989, pp. 955–972.

[4]Shaw, J., and Albion, N., "Active Control of the Helicopter Rotor for Vibration Reduction," *Journal of the American Helicopter Society*, Vol. 26, No. 4, 1981, pp. 32–39.

[5]Muller, M., Arnold, U. T. P., and Morbitzer, D., "On the Importance and Effectiveness of 2/rev IBC for Noise, Vibration and Pitch Link Load Reduction," *Proceedings of the 55th Annual Forum of the American Helicopter Society*, 2000.

[6]Bittanti, S., and Colaneri, P., "Periodic Control," *Wiley Encyclopedia of Electrical and Electronic Engineering*, edited by J. G. Webster, Wiley, New York, 1999, pp. 59–73.

[7]Johnson, W., "Self-Tuning Regulators for Multicyclic Control of Helicopter Vibration," NASA TP 1996, 1982.

[8]Gupta, N. K., and Du Val, R. W., "A New Approach for Active Control of Rotorcraft Vibration," *Journal of Guidance, Control, and Dynamics*, Vol. 5, No. 2, 1982, pp. 143–150.

[9]Du Val, R., Gregory, C., and Gupta, N., "Design and Evaluation of a State Feedback Vibration Controller," *Journal of the American Helicopter Society*, Vol. 29, No. 3, 1984, pp. 30–37.

[10]McKillip, R. M., Jr., "Periodic Control of the Individual-Blade-Control Helicopter Rotor," *Vertica*, Vol. 9, No. 2, 1995, pp. 199–225.

[11]Hall, S. R., and Wereley, N. M., "Performance of Higher Harmonic Control Algorithms for Helicopter Vibration Reduction," *Journal of Guidance, Control, and Dynamics*, Vol. 16, No. 4, 1993, pp. 793–797.

[12]Cheng, R. P., Tischler, M. B., and Celi, R., "A High-Order, Time Invariant Linearized Model for Application to HHC/AFCS Interaction Studies," *Proceedings of the 59th Annual Forum of the American Helicopter Society*, Alexandria, VA, 2003.

[13]Patt, D., Liu, L., Chandrasekar, Bernstein, D. S., and Friedmann, P. P., "The HHC Algorithm for Helicopter Vibration Reduction Revisited," *Proceedings of the 44th AIAA/ASME/ASCE/AHS/ASC Structural Dynamics and Materials Conference*, AIAA, Reston, VA, 2003.

[14]Lovera, M., Colaneri, P., and Celi, R., "Periodic Analysis of Higher Harmonic Control Techniques for Helicopter Vibration Attenuation," *Proceedings of the 2003 American Control Conference*, June 2003.

[15]Theodore, C., and Celi, R., "Helicopter Flight Dynamic Simulation with Refined Aerodynamic and Flexible Blade Modeling," *Journal of Aircraft*, Vol. 39, No. 4, 2002, pp. 577–586.

[16]Celi, R., "Hingeless Rotor Dynamics in Coordinated Turns," *Journal of the American Helicopter Society*, Vol. 36, No. 4, 1991, pp. 39–47.

[17]Lovera, M., Colaneri, P., Malpica, C., and Celi, R., "Discrete-Time, Closed-Loop Aeromechanical Stability Analysis of Helicopters with Higher Harmonic Control," 60th Annual Forum of the American Helicopter Society, June 2004.

[18]Wereley, N., and Hall, S., "Frequency Response of Linear Time Periodic Systems," *Proceedings of the 29th IEEE Conference on Decision and Control*, IEEE Publications, Piscataway, NJ, 1990, pp. 3650–3655.

[19]D'Angelo, H., *Linear Time-Varying Systems: Analysis and Synthesis*, Allyn and Bacon, Boston, 1970, pp. 193–220.

[20]Zhou, J., and Hagiwara, T., "H_2 and H_∞ Norm Computations of Linear Continuous-Time Periodic Systems via the Skew Analysis of Frequency Response Operators," *Automatica*, Vol. 38, No. 8, 2002, pp. 1381–1387.